CrossMark

RESEARCH PAPER

Differentiating *Pseudomonas* sp. strain ADP cells in suspensions and biofilms using Raman spectroscopy and scanning electron microscopy

Victoria A. Henry[1] · Julie L. P. Jessop[1] · Tonya L. Peeples[1]

Abstract High quality spectra of *Pseudomonas* sp. strain ADP in the planktonic and biofilm state were obtained using Raman microspectroscopy. These spectra enabled the identification of key differences between free and biofilm cells in the fingerprint region of Raman spectra in the nucleic acid, carbohydrate, and protein regions. Scanning electron microscopy (SEM) enabled detailed visualization of ADP biofilm with confirmation of associated extracellular matrix structure. Following extraction and Raman analysis of extracellular polymeric substances, Raman spectral differences between free and biofilm cells were largely attributed to the contribution of extracellular matrix components produced in mature biofilms. Raman spectroscopy complemented with SEM proves to be useful in distinguishing physiological properties among cells of the same species.

Keywords Raman spectroscopy · Scanning electron microscopy · Planktonic cells · Biofilm · Extracellular polymeric substances · *Pseudomona*s sp. strain ADP

Introduction

In nature, microbes often persist on surfaces in a biofilm matrix [1, 2]. Surfaces for attachment include, but are not limited to, industrial pipelines, food processing equipment, foreign material, and surfaces of artificial implants in the human body. As cells adhere to a surface and begin to multiply, they communicate with each other through a process called quorum sensing, releasing signaling molecules that enable the community to sense cell density [2, 3]. When the concentration of signaling molecules reaches a threshold, the activation of genes responsible for biosurfactant synthesis, sporulation, competence, and secretion of extracellular polymeric substances (EPS) is initiated [3]. EPS is a complex mixture of molecular components containing proteins, nucleic acids, lipids, and other biopolymers excreted by organisms, lysis, and hydrolysis of products [4, 5].

EPS makes up the major portion of the sticky extracellular matrix that surrounds cells and protects them from adverse factors such as antibiotics, protozoan grazing, and host immune response [3, 5, 6]. This protective barrier, which increases biofilm longevity, may be beneficial in bioremediation applications, but can be detrimental in the human body or in industrial applications, by causing antibiotic-resistant infections around implants and biofouling in pipes, respectively. Due to the ubiquitous nature of biofilms, there is a great interest in understanding activities within the matrix. It is apparent that the physiology of cells in biofilms may differ vastly from that of motile planktonic cells due to differences in gene expression, growth rate, and metabolism [7]. Understanding the complex nature of the biofilm may enhance current biotechnology applications and may lead to better biofilm mitigation strategies.

Raman spectroscopy provides a promising approach for gaining insight into this complex matrix of organisms in a rapid and non-destructive manner [8]. Limited sample size and preparation thereof is required, additives and dyes are not used, and varying geometries/film thicknesses can be analyzed [9, 10]. Through measurement of vibrational, rotational, and other low-frequency modes in molecules, Raman spectroscopy enables rapid identification of chemical bonds

✉ Tonya L. Peeples
tonya-peeples@uiowa.edu

[1] Department of Chemical and Biochemical Engineering, University of Iowa, 4133 Seamans Center, Iowa City, IA 52242, USA

present. Similar to confocal laser scanning microscopy, three-dimensional distributions of substances can be recorded with high spatial resolution. Raman spectroscopy can also combine both optical and spectral analyses to monitor structural and chemical changes [11]. Unlike infrared spectroscopy, Raman spectroscopy can be used in aqueous environments and generates sharper and more distinguishable bands of specific molecules [12–14]. The application of Raman spectroscopy for the analysis of biological samples is increasing because it offers the potential of non-destructive analysis and can rapidly determine cell properties with minimal expertise in molecular techniques [15, 16]. In one low resolution scan, a Raman spectrum can reveal major cellular components and their relative abundance simultaneously, without adding chemical markers [17]. Macromolecules such as nucleic acids, proteins, lipids, and carbohydrates emit strong Raman signals, thus making Raman microscopy an excellent tool for examining microbes [12]. Previously, Raman spectroscopy has been used in free-cell analysis for rapid detection and characterization of microbes, taxonomic comparison, detecting differences between populations, and analyzing composition of cells grown on morphologically differentiated cultures [8–10, 12, 15–17]. Fully hydrated biofilms have also been examined, and EPS characterization on different carriers explored [11, 18].

In this study, a comparative analysis of planktonic cells and cells in biofilms was conducted. Key Raman signals contributing to some of the biochemical properties present in biofilms were identified, and signal variations among a given bacterial species were demonstrated. Scanning electron microscopy (SEM) imaging was used to provide additional information about surface morphology and properties of the EPS matrix.

Pseudomonas sp. strain ADP was chosen for this study because of its potential bioremediation applications. Previous studies of this organism in bioreactor systems led to the discovery that these cells form biofilms [19]. ADP has the ability to metabolize atrazine, an environmental contaminant found in common herbicides, completely to ammonia and carbon dioxide through a series of hydrolytic reactions [20, 21]. The degradation pathway of ADP free cells is well established; however, there is much to learn about how ADP cells behave in a biofilm matrix to achieve enhanced remedial outcomes. In this study, ADP free cells and cells in biofilms were examined on a rich medium without the additional complication of atrazine. These initial baseline experiments provide insight into the cellular matrix in the biofilm and explore the use of Raman spectroscopy to distinguish physiological differences among cells of the same species.

Materials and methods

Cultures and reagents *Pseudomonas* sp. strain ADP was purchased from Deutsche Sammlung von Mikrooganismen und Zelkulturen (Braunschweig, Germany) and stored at −80 °C in Tryptic Soy Broth with glycerol (1:1) as a cryoprotectant. Max efficiency *Escherichia coli* Dh5α competent cells were purchased from Life Technologies (Grand Island, NY) and stored similarly to ADP. EDTA (10 mM) used for EPS extraction was purchased from Fisher Scientific (Pittsburgh, PA). Fixatives for SEM imaging, glutaraldehyde, cacodylate, osmium tetroxide, and hexamethyldisilazane (HMDS) were used as purchased from Sigma Aldrich (St. Louis, MO).

Raman analysis Spectra of free cells, biofilms, EPS, and cell pellets from biofilm were acquired using Raman microscopy to aid in identifying the corresponding chemical composition. A Thermo Nicolet Almega XR Raman spectrometer equipped with an Olympus BX 51 model microscope and Thermo Fisher Scientific OMNIC 8 software was used for Raman analysis. True confocal mode was achieved with 100 μm pinhole and a thermoelectric-cooled charged coupled device (CCD) camera with a front-illuminated open electrode format. This mode provided the means to achieve 1 μm x-y resolution and 2 μm depth resolution. Samples were illuminated with a frequency-doubled 532 nm Nd:Yv04 laser emitting approximately 10 mW laser power at the sample. Under these laser conditions, the biological samples did not burn. In addition, background fluorescence did not interfere with peak identification for chemical analysis of these samples at 532 nm, even though 785 nm is more commonly used for biological samples to avoid fluorescence typically caused by excitation at lower wavelengths. Since the intensity of the Raman shift is directly proportional to the laser wavenumber to the fourth power [22], higher quality Raman spectra with improved S/N ratio were obtained with the 532-nm laser compared to the 785-nm laser. Video images were taken by a CCD camera and stored and processed using the OMNIC 8 software.

Spectra were recorded, peaks identified, and baseline corrections for relative peak intensity ratios were processed with the OMNIC 8 software. All spectra were normalized relative to the nucleic acid peak at ∼800 cm^{-1}. Raman band assignments for free cells, biofilms, EPS, and pellets from biofilm were identified by comparison of published molecular assignments of biological samples. The relative molecular distribution in each sample was determined by calculating the relative peak intensity ratio. Three measurements, one each from three different replicates maintained under the same growth conditions, were averaged and the standard deviation and 95 % confidence interval for normal distribution were calculated. The 95 % confidence interval for normal distribution were calculated in Microsoft Excel 2013 using alpha of 0.05, sample size of 3, and standard deviation [23]. Interpretation of differences between spectra was carried out by comparing relative peak intensity ratios of constituents including nucleic acids, phenylalanine, carbohydrates, amide I, and amide III.

Free cells preparation Bacteria were thawed at room temperature, then diluted (1:10) in Luria Broth (LB) medium and grown overnight in shake flasks at 30 °C and 200 rpm. Standard LB medium as described by the American Society for Microbiology MicrobeLibrary was used during experimentation [24]. One milliliter of *E. coli* and ADP culture were inoculated separately in 9 mL of LB and incubated at 30 °C overnight with 200 rpm shaking. Overnight cell cultures in LB grew to approximately 7.0 optical density (OD_{600}), beginning with an initial 0.2 OD_{600}. Following incubation, suspended cells were centrifuged at 4 °C and $2000 \times g$ for 10 min to remove media. Cell pellets were washed three times and resuspended in sterile deionized water, and the suspension was diluted to 1.0 OD_{600} [17]. By reducing cell concentration to approximately 1.0 OD_{600}, it was easier to focus on individual cells to produce clear Raman signals without fluorescence saturating the detector.

For Raman analysis, 20 μL samples of cells in suspension were air dried onto a quartz microscope slide. Even though Raman spectroscopy can be used in aqueous environments, Raman signal-to-noise ratios were low for liquid samples due to the constant movement of cells into and out of the sampling volume during the accumulation times. Air drying cells in suspension onto quartz slides created a static environment that allowed scattered photons to be easily collected from single cells, thus producing spectra with higher signal-to-noise ratios and more easily distinguishable peaks. Using the ×10 objective with 0.25 NA, specimens were brought into focus, individual cells were magnified, and Raman spectra were collected with the ×100 objective with 0.90 NA. The accumulation time for each sample was 60 s with four accumulations, and 6th order polynomial fluorescence correction was applied. Digital images were taken through the microscope attached to the Raman spectrometer with the ×100 objective (see Fig. S1 in the Electronic Supplementary Material, ESM).

Biofilm preparation Biofilms were grown in a four-channel Teflon drip biofilm reactor made by the University of Iowa Medical Shop. Each channel had a polycarbonate lid, 0.25 μm bacterial vent, and a rubber inlet stopper. Through experimentation with different materials, Teflon was found to be best for growing biofilms since it is inert with respect to cells, thermally resistant to temperatures as high as 121 °C, and chemically resistant to detergents, acids, and bases. Standard microscope glass slides (75 mm × 25 mm × 1 mm), quartz slides (76 mm × 25 mm × 1 mm), or glass coverslips (0.13-0.16 mm thick) were placed flat on the bottom of each channel to provide a surface for cells to adhere and grow. Each chamber was inoculated with 10 mL of overnight cell broth, containing a 10 % inoculum of ADP cells suspended in LB media. The system was held in batch mode initially for 6 h to allow the cells time to adhere to each substratum. Two peristaltic Masterflex pumps with four pump heads attached were used to pump medium into each chamber for 5 days at a flow rate of 0.8 mL/min through size 13 tubing (0.8 mm ID). The reactor was kept at a 10° inclined angle to maintain steady effluent flow. Waste containers were placed 2 ft below the reactor to prevent backflow of waste material and minimize movement of exiting bacteria backward into the reactor.

Following the 5-day run, biofilms were harvested by gentle scraping and washing with sterile deionized water. For Raman analysis, biofilms were placed onto quartz microscope slides and air dried. Biofilms were viewed similarly to free cells, i.e., bringing sample into focus with the ×10 objective and then magnifying and focusing on cells with the ×100 objective (see Fig. S2 in ESM). The same exposure time and accumulation were used as for the free cells.

Tubing and associated containers were sterilized as per Tolker-Nielsen with modifications [25]. Briefly, tubing was rinsed with 0.5 % sodium hypochlorite at 4.5 mL/min for 5 min, allowing sodium hypochlorite solution to remain in the line for 2 h. Sodium hypochlorite was flushed from the system by pumping sterile deionized water through the tubing three times at 4.5 mL/min and filling the lines with air between each pass for 30 min. Sterile deionized water was then pumped through the system overnight at 0.2 mL/min. Lastly, a solution of 1 % hydrogen peroxide was pumped through tubing at 0.8 mL/min for 10 min to remove any remaining biomass. All associated glassware for feed and effluent, in addition to the biofilm reactor, were autoclaved for 20 min at 121 °C.

EPS extraction EPS was extracted as described by Sandt et al. with some modifications [11]. Briefly, biomass was separated from the culture medium by centrifugation at $2000 \times g$ for 10 min and washed three times with 0.9 % NaCl solution. The biomass was then resuspended in 10 mM EDTA (pH 8.3) at room temperature for 2 h to remove divalent cations, Ca^{2+} and Mg^{2+}, which are responsible for the crosslinking of charged compounds in the EPS matrix [26]. The biomass in solution was dialyzed against deionized water for 2 days with a 10-kDa MWCO Snakeskin® dialysis tube (ThermoScientific, Rockford IL). Dialysis removed the small molecules, leaving a solution of cells and dissociated EPS. This solution was centrifuged at $2000 \times g$ for 10 min. The resulting biomass pellet as well as the supernatant, which contained the EPS, were reserved for further analyses. For Raman analysis, 20 μL of EPS in solution was air dried onto quartz slides. Each sample was brought into focus using the ×10 objective, and data were collected using the ×100 objective. Raman spectra were obtained in a manner similar to that used for free cells. The cell pellets collected after the centrifugation of dialyzed EPS were smeared onto quartz slide and Raman spectra collected as described above.

Fixation for SEM Biofilms were grown as previously described on glass coverslips in the drip biofilm reactor. Intact biofilms on glass coverslips were placed in sterile tissue plates

and fixed for 1 h with 2.5 % glutaraldehyde in 0.1 M cacodylate buffer as described in the University of Iowa Central Microscopy Research Facility protocol [27]. Samples were rinsed in 0.1 M cacodylate buffer and further fixed with 1 % osmium tetroxide in 0.2 M cacodylate buffer to add mechanical stability and increase electron density for SEM imaging. Samples were then rinsed with distilled water and sequentially dried in ethanol. To prevent surface tension phenomena associated with ethanol evaporation, samples were immediately rinsed in hexamethyldisilazane (HMDS) to chemically dry specimens. Samples were then mounted onto aluminum stubs using silver colloidal paint and allowed to dry overnight in a desiccant. Once dried, samples were gold-palladium sputter coated to further boost the secondary electron emission of the specimen prior to examination with a Hitachi S4800 scanning electron microscope operated at 1.5 kV. SEM images were collected using ×45,000 magnification and slow scan speed. All chemicals used for fixation were handled with caution in the fume hood as described in the material safety data sheet.

Results and discussion

Original Raman spectra of ADP planktonic cells and biofilm are presented in the 600–2000 cm^{-1} fingerprint region, with putative peak assignments from published Raman spectral assignments of single bacterial cells. A high-resolution SEM image of ADP in the biofilm matrix is also presented to aid in the analysis of EPS contribution to the biofilm matrix and the interpretation of Raman data. The higher-wavenumber region (about 2800–3100 cm^{-1}), which is characteristic of lipid moieties and, specifically for Raman, strong C-H vibration modes, can also provide important information for analysis (in particular, the saturation/unsaturation degree for fatty acid moieties in cellular lipids) [28–30]. However, for the purpose of this research, higher wavenumbers are not presented for improved readability of spectra and to minimize spectral post-processing.

Free cells Raman spectra of individual ADP cells grown in liquid media were collected to compare against ADP cells grown within a biofilm. The Raman spectra obtained from a single cell in an air-dried sample contained approximately 20 sharp bands (Fig. 1B) and had higher signal-to-noise ratios than spectra from cells in liquid media. As a positive control and to compare data with published work, E. coli was also examined (Fig. 1A). Tentative band assignments for molecular components of a single cell from the literature are presented in ESM Table S1 [10–12, 15, 17, 31, 32]. The E. coli spectrum was comparable to the spectrum found in the literature [12], having most notably the Raman bands at 787, 1001, 1235, and 1667 cm^{-1}. Because a smaller spot size and more accumulations were used, a clean spectrum with high signal-

to-noise ratios was obtained. The overall shape of the spectrum is almost identical to the spectrum that has been published, with minor variation in the relative intensity of phenylalanine to carbohydrate at 1001 and 1055 cm^{-1}, respectively. Minor variations are expected when working with multicomponent systems such as cells since there are many factors such as age, growth phase, and source of nutrients that may alter spectral characteristics [15].

This Raman technique enabled the distinction between ADP and E. coli cells. Visual differences between E. coli and ADP occurred in the fingerprint regions at 747, 1126, and 1308–1392 cm^{-1} (Fig. 1), which from previous reports [11, 12, 17, 33, 34] are attributed to tryptophan, carbohydrate, and amide III content, respectively. By calculating the relative peak intensity ratios in each sample, we are able to estimate the relative amount of selected molecular components, as well as obtain a comparison that is independent of instrumental variations (Fig. 2). Theoretically, the Raman peak intensity is directly proportional to the concentration of the represented bond and thus the chemical constituents. Comparing the relative intensity ratio of tryptophan to nucleic acids (C,U) $\left(\frac{I_{747}}{I_{791}}\right)$, E. coli has a peak ratio less than half that of ADP's ratio (see Table S2 in ESM for peak ratio data). The phenylalanine to carbohydrate peak ratio $\left(\frac{I_{1001}}{I_{1124}}\right)$ for E. coli is more than two times that of ADP. The amide I to nucleic acids (A, G) content $\left(\frac{I_{1661}}{I_{1575}}\right)$ is noticeably different as well, with a relative peak ratio for E. coli that is almost two times greater than ADP. Both strains were grown on identical media and processed the same way; however, each species produces different proteins and expresses variant genes in the presence of nutrients, which hypothetically corresponds to the observed spectral differences [35, 36]. Using amide I as an indicator of peptide or protein content, these results point to higher protein to carbohydrate and protein to nucleic acid ratios on the surface of E. coli relative to ADP, when cultivated on LB media. However, the ratios for the non-polar amino acids tryptophan and phenylalanine to nucleic acid give conflicting impressions of protein to nucleic acid content. The complex microbial physiology associated with the numerous metabolites produced varies within species and growth phase [37], so differences between species are to be expected. Further work at evaluating specific protein classes might further elucidate differences between the E. coli and ADP.

Biofilm The Teflon drip biofilm reactor proved to be effective in the cultivation of mature biofilms. ADP cells grew well as a biofilm on smooth glass surfaces in the four-channel reactor (i.e., there was no need to chemically etch substrata to increase surface adhesion). After 24 h with continuous flow of media, cells began to come together and aggregate on the surface, but no extracellular matrix was visible (see Fig. S2 in ESM). By

Fig. 1 Comparison of normalized Raman spectra of (*A*) *E. coli* and (*B*) *Pseudomonas* sp. strain ADP, collected with 532 nm laser, 60 s exposure, four accumulations, and 0.6 μm spot size. Notice differences in tryptophan content at 747 cm^{-1}, reduction in phenylalanine (1001 cm^{-1}) relative to neighboring carbohydrates in ADP, and variation in relative peak intensities at 1583 and 1666 cm^{-1}
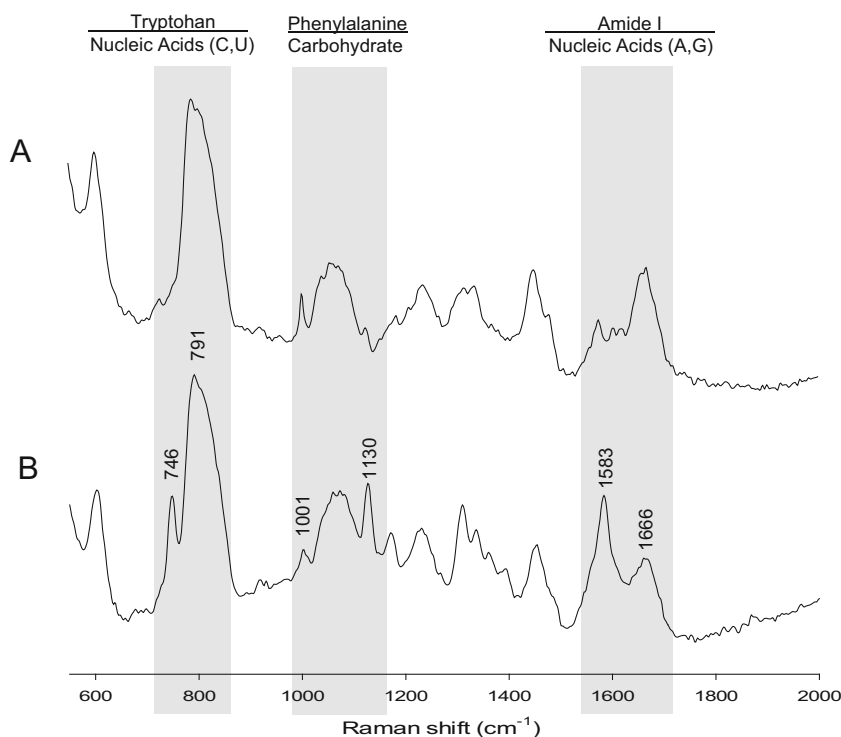
day 5, the biofilms were rich in EPS with dense webs of EPS encapsulated cells and an intricate web-like architecture (Fig. 3). Rod-shaped cells, approximately 1.0–2.0 μm in length, produced elongated EPS fibers that coated cell exteriors, bound neighboring cells together, and formed micro structures within open terrestrial spaces between cells. These mats of biomass with open channels are consistent with the definition of a mature biofilm [38].

Raman analysis of mature biofilms revealed similarities to free cells in regards to molecular compounds present, but with differences in molecular distribution (Fig. 4). When comparing relative peak intensity ratios (Fig. 5) in the tryptophan to nucleic acid region $\left(\frac{I_{752}}{I_{789}}\right)$, ADP biofilms have a ratio two

times higher than that for free cells (see Table S3 in ESM for peak intensity data). The biofilm matrix can act as a recycling center, retaining lysed cell components and stabilizing the activity of extracellular enzymes [5, 39]. On the other hand, the peak ratios of phenylalanine to carbohydrates $\left(\frac{I_{1008}}{I_{1132}}\right)$, lipids to amide III $\left(\frac{I_{1455}}{I_{1313}}\right)$, and amide I to nucleic acids (A, G) $\left(\frac{I_{1672}}{I_{1586}}\right)$ are comparable in both the free cell and biofilm, suggesting similar abundances of molecular components in those regions. The simultaneous increase in DNA content and protein in the biofilm could plausibly explain why the relative peak intensity ratio of amide I to nucleic acids was comparable in both the free cell and biofilm. Biofilms have
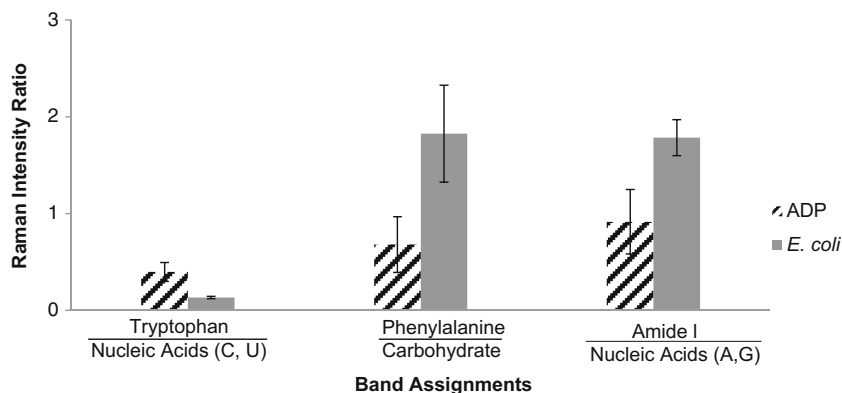

Fig. 2 Relative Raman intensities peak ratios of ADP in comparison to *E. coli*. Three replicates of each sample with 95 % confidence interval bars displayed. Notable difference is present in the tryptophan to nucleic acid (C, U) region (I_{747}/I_{791}). Some differences are also detected in the phenylalanine to carbohydrate (I_{1001}/I_{1124}) and amide I to nucleic acids (A,G) regions (I_{1661}/I_{1575}). See ESM Table S2 for actual peak ratio values
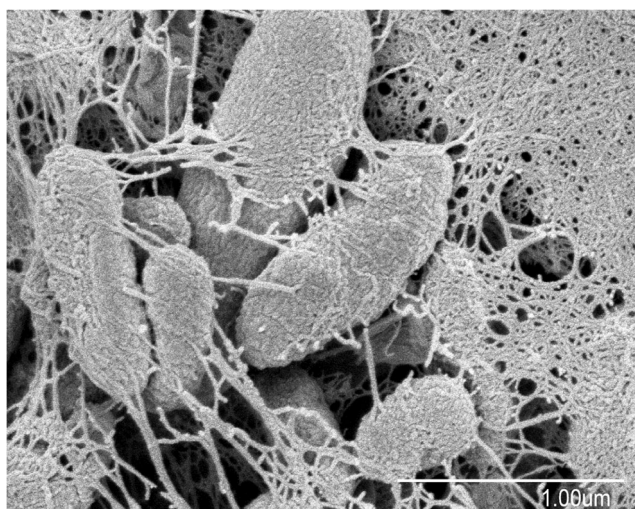
Fig. 3 SEM image of 5-day-old *Pseudomonas* sp. strain ADP biofilm with 15,000 magnification. Extracellular polymeric substances dominate the biofilm matrix, creating web-like structure surrounding cells and spreading throughout the matrix creating an intricate architecture

been reported to have higher extracellular protein content than free cells due to protein assistance with the architecture and formation of biofilms [39]. In addition, there is increased access to genetic material remaining entrapped in the matrix.

EPS contribution To aid in understanding the Raman spectra of cells in mature biofilms, EPS was extracted, and both EPS and the remaining cell pellets were spectrally examined. In the SEM image of the mature biofilm, EPS appeared to be the dominating component (Fig. 3). SEM imaging of the 5-day-old biofilm showed masses of EPS adhered closely to cells, producing dense web-like structures within the matrix. Raman analysis of EPS confirmed that the biofilm signal (Fig. 4B) may largely be attributed to EPS (Fig. 4C). However, the presence of EPS was not the sole reason for chemical differences between the biofilm and free cell spectra. Both EPS and the biofilm have peak ratios for tryptophan to nucleic acids (U, G) $\left(\frac{I_{752}}{I_{794}}\right)$ greater than the same ratio for the free cells, 31 and 51 % higher, respectively (Fig. 5). The relative peak intensity ratios of phenylalanine to carbohydrate $\left(\frac{I_{1006}}{I_{1130}}\right)$ are comparable in EPS and the biofilm. However, there is a 31 % difference in amide I to nucleotides relative peak intensity ratio $\left(\frac{I_{1669}}{I_{1588}}\right)$ between EPS and the biofilm. Among the free cell, biofilm, and EPS spectra, amide I was most prominent in EPS as expected due to the abundance of extracellular proteins present as explained earlier. Also, after adding the free cell spectrum to the EPS spectrum, the resulting spectrum was very similar to the cell in biofilm spectrum (see Fig. S3 in ESM). These results suggest that EPS secretion contributed to, but is not the sole reason, for chemical differences between the biofilm and free cell spectra.

Pellets The Raman spectra of cell pellets remaining after EPS extraction from the biofilm were collected to determine how the molecular distribution of cellular components varied when cells were grown in a biofilm rather than motile planktonic cells (Fig. 4D). The tryptophan to nucleic acid (C,U) region $\left(\frac{I_{750}}{I_{799}}\right)$ is 30 % lower in pellets removed from the EPS matrix than free cells from the liquid suspension (Fig. 5). The phenylalanine to carbohydrate peak intensity ratio $\left(\frac{I_{1006}}{I_{1130}}\right)$ is 19 % higher in pellets than free cells. The amide I to nucleotides (A, G) content $\left(\frac{I_{1672}}{I_{1586}}\right)$ is almost twice as high in pellets. One possible explanation for these notable differences could be the regulation of gene expression in response to increased cell density. Some bacteria have the ability to sense the density of their species in the culture environment and then respond by coordinating the expression of genes related to EPS secretion [3]. Due to several factors, including growth conditions, cell-cell communication, and gene regulation, cells from the mature biofilm behave differently than motile planktonic cells, which were evident in Raman spectra and captured in the peak ratio calculations [37, 39].

Conclusion and future perspectives

By visual inspection of Raman spectra and comparison of relative peak intensity ratios, it is possible to detect differences in molecular component distributions of ADP free cells and ADP biofilms. Superior Raman spectra of microbes were obtained by removing water from samples, (thereby increasing concentration), using a 532-nm laser to induce the Raman effect, and increasing sample accumulation time. This analytical approach was validated by comparing experimental Raman spectra of *E. coli* with published spectra.

Free cells of *E. coli* and ADP showed differences in relative peak intensity ratios greater than twofold. Cells of the same species, grown differently (i.e., freely in suspension or in biofilm) showed differences in nucleic acid, carbohydrate, and protein content in the fingerprint region. Following SEM imaging and EPS extraction from mature biofilms, differences were largely attributed to the presence of EPS in the matrix.

Moving forward, EPS will be separated into three fractions, soluble EPS, lightly bound EPS, and tightly bound EPS, for Raman analysis. Molecular component analysis of EPS by peak identification and relative distribution will more precisely determine EPS contribution to the biofilm matrix. EPS properties significantly influence the physicochemistry of microbial aggregates, including adsorption ability, surface charge, structure, and hydrophobicity [18]. Success of this research will ultimately lead to a firmer grasp of scientific fundamentals associated with microbial biofilms and aid in the building of the Raman microbial library.

Fig. 4 Normalized Raman spectra of *Pseudomonas* sp. strain ADP without baseline correction, collected with 532 nm laser, 60 s exposure, and 0.6 μm spot size: (*A*) free cell; (*B*) biofilm; (*C*) extracted extracellular polymeric substance; and (*D*) remaining pellets from biofilm. Notice change in relative intensity of peaks in tryptophan/nucleic acid region (C,U) and phenylalanine/carbohydrate region. Spectra B and C have almost the same curve, with the exception of the amide III region, indicating that EPS is a dominating feature in a mature biofilm. Dissimilarities revealed in spectra A and D show that EPS is not the sole contributing factor to differences between biofilm and planktonic microbes
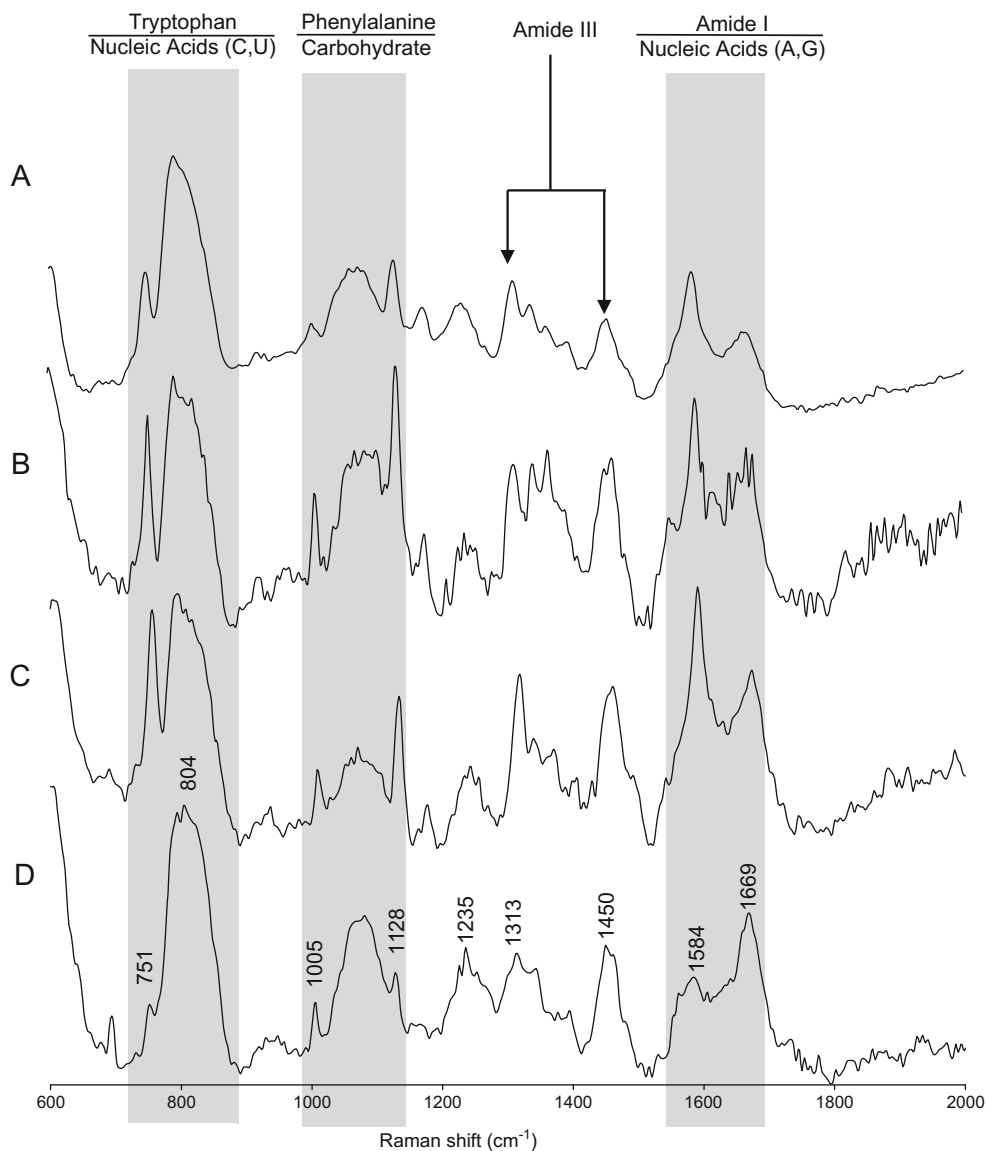

Fig. 5 Relative Raman intensities peak ratios of *Pseudomonas* sp. strain ADP free cell, biofilm, EPS, and pellets remaining after EPS extraction. Triplicates of each sample, with 95 % confidence intervals bars, are presented. See ESM Table S3 for actual peak ratios values of tryptophan to nucleic acid (I_{746}/I_{789}), phenylalanine to carbohydrate (I_{1002}/I_{1127}), and amide I to nucleic acids (A,G) region (I_{1663}/I_{1582})
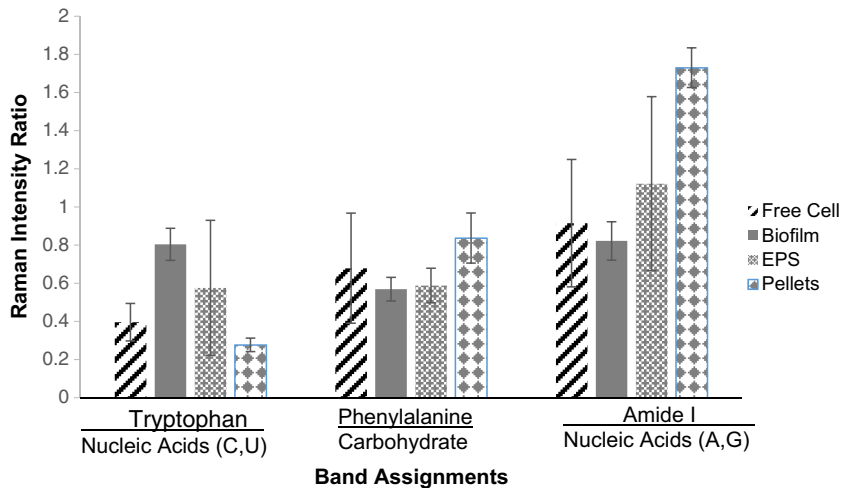
Compliance with ethical standards

Conflict of interest The authors declare that they have no conflict of interest.

References

1. Castro L, Zhang R, Munoz JA, Gonzalez F, Blazquez LM, Sand W, et al. Characterization of exopolymeric substances (EPS) produced by *Aeromonas hydrophila* under reducing conditions. Biofouling. 2014;30(4):501–11.

2. Shrout JD, Tolker-Nielsen T, Givskov M, Parsek MR. The contribution of cell-cell signaling and motility to bacterial biofilm formation. MRS Bull. 2011;36(5):367–73.

3. Nadell CD, Xavier JB, Levin SA, Foster KR. The evolution of quorum sensing in bacterial biofilms. PLoS Biol. 2008;6(1):171–9.

4. Sheng GP, Yu HQ, Li XY. Extracellular polymeric substances (EPS) of microbial aggregates in biological wastewater treatment systems: a review. Biotechnol Adv. 2010;28(6):882–94.

5. Flemming HC, Wingender J. The biofilm matrix. Nat Rev Microbiol. 2010;8(9):623–33.

6. Pamp SJ, Gjermansen M, Tolker-Nielsen T. The biofilm matrix: a sticky framework. In: Kjelleberg S, Givskov M, editors. The biofilm mode of life: mechanisms and adaptations. UK: Horizon Bioscience; 2007. pp. 37–69.

7. Mikkelsen H, Duck Z, Lilley KS, Welch M. Interrelationships between colonies, biofilms, and planktonic cells of *Pseudomonas aeruginosa*. J Bacteriol. 2007;189(6):2411–6.

8. Patzold R, Keuntje M, Anders-von AA. A new approach to nondestructive analysis of biofilms by confocal Raman microscopy. Anal Bioanal Chem. 2006;386(2):286–92.

9. Choo-Smith LP, Maquelin K, van Vreeswijk T, Bruining HA, Puppels GJ, Ngo Thi NA, et al. Investigating microbial (micro)colony heterogeneity by vibrational spectroscopy. Appl Environ Microbiol. 2001;67(4):1461–9.

10. Wagner M, Ivleva NP, Haisch C, Niessner R, Horn H. Combined use of confocal laser scanning microscopy (CLSM) and Raman microscopy (RM): investigations on EPS-matrix. Water Res. 2009;43(1):63–76.

11. Sandt C, Smith-Palmer T, Pink J, Brennan L, Pink D. Confocal Raman microspectroscopy as a tool for studying the chemical heterogeneities of biofilms in situ. J Appl Microbiol. 2007;103(5):1808–20.

12. Huang WE, Griffiths RI, Thompson IP, Bailey MJ, Whiteley AS. Raman microscopic analysis of single microbial cells. Anal Chem. 2004;76(15):4452–8.

13. Abu-Absi NR, Kenty BM, Cuellar ME, Borys MC, Sakhamuri S, Strachan DJ, et al. Real time monitoring of multiple parameters in mammalian cell culture bioreactors using an in-line Raman spectroscopy probe. Biotechnol Bioeng. 2011;108(5):1215–21.

14. Li B, Ryan PW, Ray BH, Leister KJ, Sirimuthu NMS, Ryder AG. Rapid characterization and quality control of complex cell culture media solutions using Raman spectroscopy and chemometrics. Biotechnol Bioeng. 2010;107(2):290–301.

15. Maquelin K, Kirschner C, Choo-Smith LP, van den Braak N, Endtz HP, Naumann D, et al. Identification of medically relevant microorganisms by vibrational spectroscopy. J Microbiol Methods. 2002;51(3):255–71.

16. Mobili P, Londero A, De Antoni G, Gomez-Zavaglia A, Araujo-Andrade C, Avila-Donoso H, et al. Multivariate analysis of Raman spectra applied to microbiology. Discrimination of microorganisms at the species level. Rev Mex de Fis. 2010;56(5):378–85.

17. Schuster KC, Reese I, Urlaub E, Gapes JR, Lendl B. Multidimensional information on the chemical composition of single bacterial cells by confocal Raman microspectroscopy. Anal Chem. 2000;72(22):5529–34.

18. Chen YP, Zhang P, Guo JS, Fang F, Gao X, Li C. Functional groups characteristics of EPS in biofilm growing on different carriers. Chemosphere. 2013;92(6):633–8.

19. Biglione NK. Fundamental kinetic parameters of suspended and biofilm atrazine degrading cells [dissertation]. The University of Iowa; 2007.

20. Martinez B, Tomkins J, Wackett LP, Wing R, Sadowsky MJ. Complete nucleotide sequence and organization of the atrazine catabolic plasmid pADP-1 from *Pseudomonas* sp. strain ADP. J Bacteriol. 2001;183(19):5684–97.

21. Govantes F, Garcia-Gonzalez V, Porrua O, Platero AI, Jimenez-Fernandez A, Santero E. Regulation of the atrazine-degradative genes in *Pseudomonas* sp. strain ADP. FEMS Microbiol Lett. 2010;310(1):1–8.

22. Ingle JD, Crouch SR. Spectrochemical analysis. Englewood Cliffs, NJ: Prentice Hall; 1988. p. pp. 501.

23. Carlberg CG. Statistical analysis: Microsoft Excel 2010. Indianapolis: Que; 2011.

24. MacWilliams MP, Liao MK. Luria broth (LB) and Luria agar (LA) media and their uses protocol: American Society for Microbiology MicrobeLibrary. 2006. http://www.microbelibrary.org/component/resource/laboratory-test/3031-luria-broth-lb-and-luria-agar-la-media-and-their-uses-protocol. Accessed 20 Jan 2012.

25. Tolker-Nielsen T, Sternberg C. Growing and analyzing biofilms in flow chambers. Curr Protoc Microbiol. 2011;21:1B.2.1–1B.2.17.

26. Nielsen PH, Jahn A. Extraction of EPS. In: Wingender J, Neu TR, Flemming HC, editors. Microbial extracellular polymeric substances. Berlin Heidelberg: Springer; 1999. pp. 49–72.

27. The University of Iowa Central Microscopy Research Facility. Scanning electron microscopy. http://cmrf.research.uiowa.edu/scanning-electron-microscopy. Accessed 15 Oct 2013.

28. Czamara K, Majzner K, Pacia MZ, Kochan K, Kaczor A, Baranska M. Raman spectroscopy of lipids: a review. J Raman Spectrosc. 2015;46(1):4–20.

29. Kamnev AA, Tarantilis PA, Antonyuk LP, Bespalova LA, Polissiou MG, Colina M, et al. Fourier transform Raman spectroscopic characterisation of cells of the plant-associated soil bacterium *Azospirillum brasilense* Sp7. J Mol Struct. 2001;563:199–207.

30. Naumann D, Keller S, Helm D, Schultz C, Schrader B. FT-IR spectroscopy and FT-Raman spectroscopy are powerful analytical tools for the non-invasive characterization of intact microbial cells. J Mol Struct. 1995;347:399–405.

31. Ude S, Bailey MJ, Huang WE, Spiers AJ. The environmental plasmid pQBR103 alters the single-cell Raman spectral profile of *Pseudomonas fluorescens* SBW25. Microb Ecol. 2007;53(3):494–7.

32. Schwartz T, Jungfer C, Heißler S, Friedrich F, Faubel W, Obst U. Combined use of molecular biology taxonomy, Raman spectrometry, and ESEM imaging to study natural biofilms grown on filter materials at waterworks. Chemosphere. 2009;77(2):249–57.

33. Xie C, Li YQ, Tang W, Newton RJ. Study of dynamical process of heat denaturation in optically trapped single microorganisms

by near-infrared Raman spectroscopy. J Appl Phys. 2003;94(9): 6138–42.

34. Li-Chan ECY. The applications of Raman spectroscopy in food science. Trends Food Sci Technol. 1996;7(11):361–70.

35. Stockel S, Kirchhoff J, Neugebauer U, Rosch P, Popp J. The application of Raman spectroscopy for the detection and identification of microorganisms. J Raman Spectrosc. 2016;47:89–109.

36. Busse HJ, Denner EBM, Lubitz W. Classification and identification of bacteria: current approaches to an old problem. Overview of methods used in bacterial systematics. J Biotechnol. 1996;47(1):3–38.

37. Eboigbodin KE, Biggs CA. Characterization of the extracellular polymeric substances produced by *Escherichia coli* using infrared spectroscopic, proteomic, and aggregation studies. Biomacromolecules. 2008;9:686–95.

38. Apicella MA, Shao J, Neil RB. Methods for studying *Neisseria meningitidis* biofilms. In: Christodoulides, editor. *Neisseria meningitidis*: advanced methods and protocols. New York: Springer; 2012. pp. 169–184.

39. Wu S, Baum MM, Kerwin J, Guerrero D, Webster S, Schaudinn C, et al. Biofilm-specific extracellular matrix proteins of nontypeable *Haemophilus influenzae*. Pathog Dis. 2014;72(3):143–60.